nature neuroscience

UNC119 is required for G protein trafficking in sensory neurons

Houbin Zhang[1,10], Ryan Constantine[1,2,10], Sergey Vorobiev[3], Yang Chen[3], Jayaraman Seetharaman[3], Yuanpeng Janet Huang[4], Rong Xiao[4], Gaetano T Montelione[4], Cecilia D Gerstner[1], M Wayne Davis[5], George Inana[6], Frank G Whitby[7], Erik M Jorgensen[5,8], Christopher P Hill[7], Liang Tong[3] & Wolfgang Baehr[1,5,9]

UNC119 is widely expressed among vertebrates and other phyla. We found that UNC119 recognized the acylated N terminus of the rod photoreceptor transducin α (Tα) subunit and *Caenorhabditis elegans* G proteins ODR-3 and GPA-13. The crystal structure of human UNC119 at 1.95-Å resolution revealed an immunoglobulin-like β-sandwich fold. Pulldowns and isothermal titration calorimetry revealed a tight interaction between UNC119 and acylated Gα peptides. The structure of co-crystals of UNC119 with an acylated Tα N-terminal peptide at 2.0 Å revealed that the lipid chain is buried deeply into UNC119's hydrophobic cavity. UNC119 bound Tα-GTP, inhibiting its GTPase activity, thereby providing a stable UNC119–Tα-GTP complex capable of diffusing from the inner segment back to the outer segment after light-induced translocation. UNC119 deletion in both mouse and *C. elegans* led to G protein mislocalization. Thus, UNC119 is a Gα subunit cofactor essential for G protein trafficking in sensory cilia.

Non-motile primary cilia sensitive to external stimuli are found in various animal sensory neurons. In mammalian photoreceptors or *C. elegans* olfactory cells, light receptors (rhodopsin) or odorant receptors, together with their G proteins and associated signal transduction components, are transported to cilia by vesicular and intraflagellar mechanisms. Defects in these trafficking pathways have been shown to impair signal transduction, ciliogenesis and cilia maintenance[1], often leading to severe disease. For both photoreceptors and odorant receptors, evidence continues to emerge of an ever-increasing number of polypeptides involved in vesicular trafficking and stabilizing intraflagellar transport, including components of the BBSome[2], Rab GTPases[3], Arf and Arf-like GTPases[4] and prenyl-binding proteins[5].

UNC119 is a 27-kDa polypeptide identified in the basal body proteome of *C. reinhardtii*[6], the flagellar rootlet of *Naegleria gruberi*[7], neurons of *C. elegans*[8] and the mouse photoreceptor sensory cilium complex[9]. *unc-119* was first discovered in *C. elegans* on the basis of a spontaneous mutation affecting locomotion, feeding behavior and chemosensation[8]. Independently, a protein named retina gene 4 (RG4) was discovered in the retina and recognized to be a *C. elegans unc-119* ortholog[10]. Although expressed in multiple tissues, UNC119 predominates in retinal photoreceptor inner segments and synaptic regions[11–13]. UNC119 has been shown to interact with several diverse proteins, including the Arf-like GTPases ARL2 (ref. 14) and ARL3 (ref. 15); the Ca^{2+}-binding protein CaBP4, a modulator of the voltage-gated Ca^{2+} channel Ca_v 1.4 present in rod and cone synapses[16]; and the synaptic ribbon component RIBEYE[17] of photoreceptors. A heterozygous stop codon (K57ter) identified in the human *UNC119* gene of an individual with late-onset dominant cone dystrophy also produced dominant dystrophy in a transgenic mouse model[18].

Apart from the mammalian retina, UNC119 has been detected in leukocytes (eosinophils), T cells, lung fibroblasts[19], the adrenal glands, cerebellum and kidney[11]. UNC119 has also been shown to activate Src-type tyrosine kinases associated with the interleukin-5 receptor and the T-cell receptor by interacting with them through Src homology domains located in its N-terminal half[20]. Widespread distribution of UNC119 in vertebrates, invertebrates and even flagellated protozoa suggests that it is highly conserved and has multiple functions throughout the animal kingdom.

We identified UNC119 as a lipid-binding protein interacting with acylated N termini of G protein α subunits present in mouse photoreceptors and *C. elegans* olfactory neurons. The crystal structure at 1.95-Å resolution revealed that UNC119 adopts an immunoglobulin-like β-sandwich fold. The N-terminal peptide of Tα inserts deeply into the hydrophobic cavity formed by the β-sandwich fold of UNC119. Notably, the ligand enters the protein interior from the opposite side of that seen for structurally related proteins, and the first six amino acid residues of the Tα peptide are buried in the core, making intimate contacts with UNC119. Using UNC119 knockouts, we found that UNC119 is required for G protein trafficking in animal models as diverse as mouse and *C. elegans*.

[1]Department of Ophthalmology, University of Utah Health Science Center, Salt Lake City, Utah, USA. [2]Graduate Program in Neuroscience, University of Utah Health Science Center, Salt Lake City, Utah, USA. [3]Department of Biological Sciences, Northeast Structural Genomics Consortium, Columbia University, New York, New York, USA. [4]Center for Advanced Biotechnology and Medicine, Department of Molecular Biology and Biochemistry, Northeast Structural Genomics Consortium, Rutgers University, Piscataway, New Jersey, USA. [5]Department of Biology, University of Utah, Salt Lake City, Utah, USA. [6]Bascom Palmer Eye Institute, University of Miami Miller School of Medicine, Miami, Florida, USA. [7]Department of Biochemistry, University of Utah School of Medicine, Salt Lake City, Utah, USA. [8]Howard Hughes Medical Institute, University of Utah, Salt Lake City, Utah, USA. [9]Department of Neurobiology and Anatomy, University of Utah Health Science Center, Salt Lake City, Utah, USA. [10]These authors contributed equally to this work. Correspondence should be addressed to W.B. (wbaehr@hsc.utah.edu).

Received 28 February; accepted 14 April; published online 5 June 2011; doi:10.1038/nn.2835

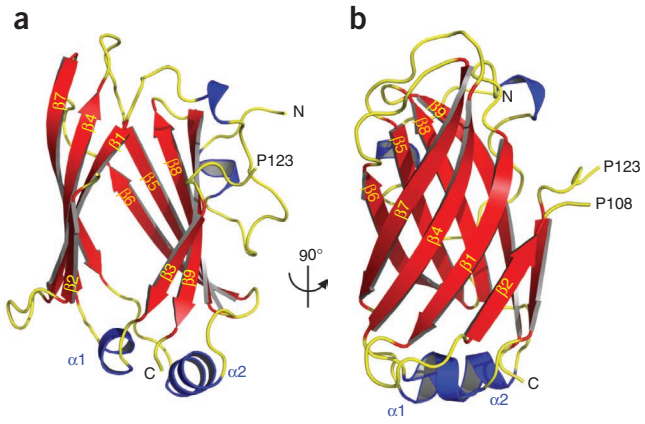

Figure 1 Crystal structure of human UNC119. (**a**) Ribbon representation of the structure of human UNC119 (residues 57–237). Nine β strands (β1–β9), shown in red, create two β sheets that splay apart at one end to create an opening to the cavity at the center of the β sandwich. The N and C termini are marked N and C, respectively. The structure of the loop 108–123 connecting strands β2 and β3 could not be resolved. (**b**) Structure of UNC119 viewed after a 90° rotation around the vertical axis.

RESULTS

The structure of human UNC119 at 1.95-Å resolution

The crystal structure of human UNC119 (residues 57–237) at 1.95-Å resolution (PDB ID: 3GQQ) contains an immunoglobulin-like β-sandwich fold comprised of two β sheets (**Figs. 1a**,**b**). The β sheets, arranged in four antiparallel strands, fold in a Greek key pattern (**Supplementary Fig. 1a**), which is found in a large number of diverse proteins[21]. Strands β3-β4 and β7-β8 are linked by short α-helical loops (α1 and α2 in **Fig. 1a**). In the UNC119 structure, the two sheets are splayed apart from each other at one edge of this β sandwich, revealing a narrow, deep cavity penetrating the center of this structure (**Fig. 1a**). The atomic model is consistent with the crystallographic data and expected stereochemistry (**Supplementary Table 1**).

A search of the Protein Data Bank with the program DaliLite (http://www.ebi.ac.uk/Tools/dalilite/index.html) returned a large number of similar structures, including PrBP/δ (*Z* score 12, 24% overall amino acid sequence identity with UNC119) and Rho-GDP dissociation inhibitor 1 (RhoGDI, *Z* score 9, 10% overall identity) (**Supplementary Figs. 1b** and **2a**). When restricted to the region that folds into β sheets, UNC119 sequence similarity with PrBP/δ increased to 56% (**Supplementary Fig. 1c**). PrBP/δ is a prenyl-binding protein that interacts with prenylated proteins participating in phototransduction[5], whereas RhoGDI regulates the function of the Rho GTPase CDC42 (ref. 22). Both proteins possess a hydrophobic pocket capable of accommodating farnesyl and geranylgeranyl chains[23,24]. The aforementioned structural similarities suggest that UNC119 might be a lipid-binding protein.

UNC119 interacts with the transducin-α subunit

To identify interacting partners of UNC119 in photoreceptors, we used GST fusion protein pulldown followed by high-performance liquid chromatography and tandem mass spectrometry (LC-MS/MS). From bovine retina lysates, we identified a polypeptide of approximately 40 kDa that specifically bound GST-UNC119 (**Fig. 2a**). Sequence identification by LC-MS/MS yielded numerous peptides matching the rod Tα subunit and one matching cone Tα (**Fig. 2b**), both of which are involved in phototransduction. In the inactive state, GDP is bound to Tα, permitting the interaction with the transducin subunits Tβγ, yielding the heterotrimeric complex, Tαβγ. To test whether UNC119 pulled down the heterotrimeric complex through its interaction with Tα, pulldowns were repeated using wild-type and *Gnat1*$^{-/-}$ (Tα knockout) mouse retina lysates (**Fig. 2c**). Immunoblots probed with antibodies to Tα and Tγ revealed that UNC119 interacts with Tα, but not with farnesylated Tγ (**Fig. 2c**). Pulldowns were negative using *Gnat1*$^{-/-}$ retina lysates (**Fig. 2c**), confirming that UNC119 is not a prenyl-binding protein.

The glycine residue at the N terminus of rod Tα (G2) is heterogeneously acylated[25], carrying either C12:0, C14:1, C14:2 or C14:0 side chains, which are important for targeting Tα to the outer segment[26]. Given the structural similarity among UNC119, PrBP/δ and RhoGDI, we suspected that UNC119 would interact with the N-terminal acyl group of Tα. To test this hypothesis, we replaced G2 at the N terminus of Tα with alanine, which prevents Tα acylation. Recombinant

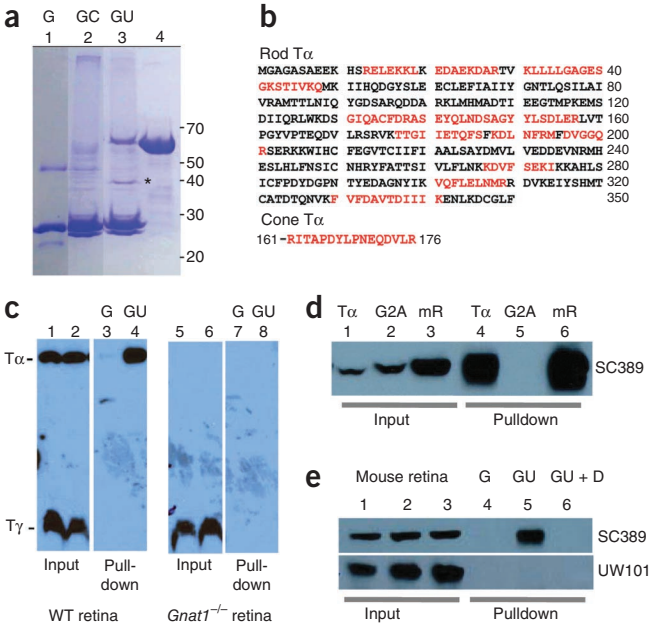

Figure 2 Interaction of UNC119 with Tα polypeptides. (**a**) Pulldown of rod and cone Tα with GST-UNC119 (representative Coomassie-stained gel of four independent experiments). Bound polypeptides from bovine retina lysates were analyzed by SDS-PAGE (lane 1, recombinant GST (G); lane 2, pulldown with GST as a control (GC); lane 3, GST-UNC119 pulldown (GU); lane 4, GST-UNC119 fusion protein). An asterisk identifies the proteins pulled down by GST-UNC119. (**b**) Identification of peptides by LC-MS/MS. The 40-kDa polypeptides pulled down with GST-UNC119 were identified by LC-MS/MS. Identified peptide sequences, shown in red, were matched with rod and cone Tα. (**c**) GST-UNC119 pulldown of Tα from wild-type (WT, lanes 1–4) and *Gnat1*$^{-/-}$ retinas (lanes 5–8). Lanes 1, 2, 5 and 6, input; lanes 3 and 7, control pulldowns with GST; lanes 4 and 8, pulldowns with GST-UNC119. Acylated Tα was pulled down (lane 4), but not farnesylated Tγ (lane 8). (**d**) GST-UNC119 pulldown of Tα and Tα(G2A) expressed in HEK cells (lanes 1–3, input; lanes 4–6, pulldowns; lanes 1 and 4, HEK cells expressing bovine Tα; lanes 2 and 5, HEK cells expressing bovine Tα(G2A); lanes 3 and 6, mouse retina lysates). Blot was probed with antibody to Tα. Note that UNC119 does not interact with non-acylated Tα(G2A). (**e**) Specificity of retina lysate pulldowns (lanes 1–3, mouse retina lysates (input); lanes 4–6, retina lysate pulldowns; lane 4, GST control; lane 5, 10 μg GST-UNC119 was added; lane 6, 10 μg GST-UNC119 with 0.1% Triton X-100 and 0.1% NP-40 (DT) present in the binding buffer). Top, blot probed with antibody to Tα. Bottom, same blot probed with antibody to GCAP1. Note that myristoylated GCAP1 does not interact with GST-UNC119.

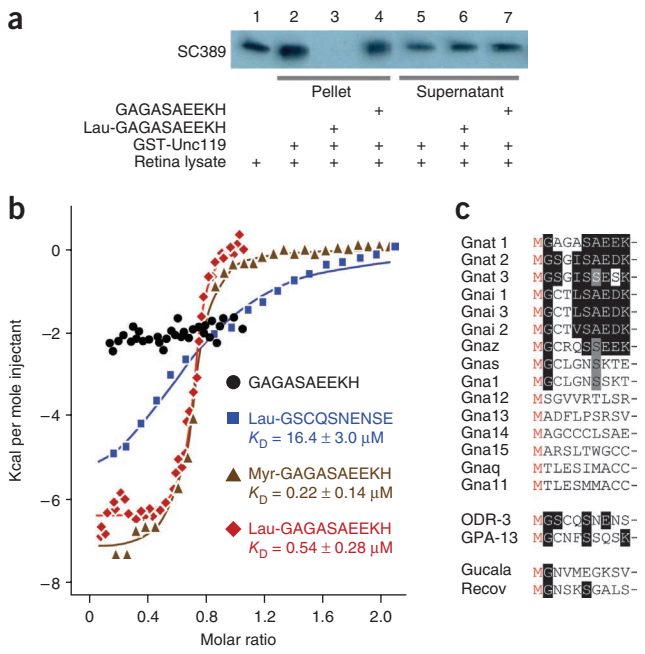

Figure 3 UNC119 is an acyl-binding protein. (**a**) GST-UNC119 pulldowns and inhibition by an acylated N-terminal Tα peptide (lane 1, retina lysate; lanes 2–4, glutathione bead pellets of retina lysates that were incubated with GST-UNC119, in the absence of peptide (lane 2), the presence of lauroyl-GAGASAEEKH (lane 3), and in the presence of non-acylated GAGASAEEKH peptide (lane 4); lanes 5–7, supernatants of 2–4). Note that lauroyl-GAGASAEEKH competed for binding (lane 3), but the non-acylated peptide did not (lane 4). (**b**) ITC. Human UNC119 was titrated with G protein α subunit N-terminal peptides. Red symbols, titration with N-terminal Tα peptide (lauroyl-GAGASAEEKH); black circles, titration with non-lauroylated GAGASAEEKH; green triangles, titration with myristoylated GAGASAEEKH; blue squares, titration with ODR-3 N-terminal peptide lauroyl-GSCQSNENSE. Lauroyl-GAGASAEEKH (red) and myristoyl-GAGASAEEKH (green) peptides were fit to a one-site model and bound with K_D values of 0.54 ± 0.28 μM and 0.22 ± 0.14 μM, respectively. Lauroyl–ODR-3 (blue) binding was more than one order of magnitude weaker (16.4 ± 3.0 μM). (**c**) Alignment of N-terminal peptides of mouse G protein α subunits, *C. elegans* G protein α subunits GPA-13 and ODR-3, and Ca^{2+}-binding proteins GCAP1, GCAP2 and recoverin. Peptides lacking Gly at position 2 cannot be myristoylated, therefore interaction with UNC119 through an acyl chain does not extend to all subfamilies of Gα.

Tα(G2A) did not interact with bovine GST-UNC119 in pulldown assays (**Fig. 2d**), suggesting that the acyl side chain attached to G2 of Tα mediates the interaction with GST-UNC119. Furthermore, UNC119 failed to interact with N-myristoylated GCAP1 (**Fig. 2e**) or recoverin (data not shown), suggesting that the interaction with UNC119 requires some degree of specificity.

UNC119 is an acyl-binding protein

To independently confirm that UNC119 is an acyl-binding protein, we added a synthetic lauroylated (C12:0) peptide corresponding to the N terminus of bovine Tα (2-GAGASAEEKH-11) to the pulldown assay. The acylated Tα peptide was able to competitively inhibit binding of Tα to UNC119 (**Fig. 3a**), whereas the unacylated peptide had no effect (**Fig. 3a**). These results support the requirement for the N-terminal acyl group as a mediator of the interaction between Tα and UNC119.

We then employed isothermal titration calorimetry (ITC) to determine the binding constant of acylated N-terminal G protein α subunit peptides with UNC119 (**Fig. 3b**). ITC measures the binding enthalpy of two reactants enabling the resolution of two or more binding sites. We titrated the acylated N-terminal bovine Tα peptides and the acylated N-terminal *C. elegans* ODR-3 peptide (GSCQSNENSE). ODR-3 is expressed in *C. elegans* AWA, AWB and AWC olfactory neurons and participates in chemosensory signal transduction (the *unc-119* null mutation was originally discovered in *C. elegans*)[8]. Microcalorimetry experiments showed that the unacylated Tα peptide does not interact with recombinant human UNC119, whereas lauroyl- and myristoyl-GAGASAEEKH each exhibited tight binding at a single site with K_D values of approximately 0.54 ± 0.28 μM and 0.22 ± 0.14 μM, respectively (**Fig. 3b**). This dissociation constant is similar to those measured *in vitro* for farnesyl and geranylgeranyl side chains with PrBP/δ (0.7 μM and 19 μM, respectively)[24]. UNC119 also bound the lauroylated N-terminal peptide derived from ODR-3, but the interaction was two orders of magnitude weaker than that of the lauroyl Tα peptide (K_D = 16.4 ± 3.0 μM), further implicating the N-terminal residues in binding specificity. Alignment of mouse N-terminal Gα peptides revealed that the *Gna11-15* and *Gnaq* subfamilies are not N-terminally acylated (**Fig. 3c**), indicating that the UNC119-Gα subunit interaction does not extend to all Gα subfamilies.

The UNC119 hydrophobic cavity is the lipid binding site

Interpretation of our structural and biochemical results suggest that the lipid inserts into the hydrophobic cavity at the center of the β sandwich. The co-crystal structure of UNC119 with the lauroylated Tα peptide at 2.0 Å (PDB ID: 3RBQ) showed that the pocket easily accommodates a lauroyl (C12) moiety (**Fig. 4**) in a very specific fashion, as each molecule in the asymmetric unit of the crystal contains a similarly bound ligand (**Supplementary Table 2** and **Supplementary Fig. 3**). The cavity is lined predominantly by hydrophobic residues (mostly Phe and Tyr) that mediate the interaction with the lauroylated Tα peptide primarily via van der Waals forces, consistent with the properties of a lipid-binding site (**Fig. 4c** and **Supplementary Fig. 2c**). Notably, entrances to the lipid-binding sites of PrBP/δ and RhoGDI (**Supplementary Fig. 1b**) do not exist in UNC119, but instead are found on the opposite edge of the β sandwich (**Fig. 4a**,**b** and **Supplementary Fig. 2a**,**b**).

The lauroyl group and the first six residues of the Tα peptide are buried in the hydrophobic pocket of UNC119 (**Fig. 4c** and **Supplementary Fig. 2c**), whereas peptide residues 7–10 make only peripheral contact with UNC119 and are poorly ordered. In general, the surrounding protein residues formed a surface that is highly complementary to the shape of the ligand, thereby rationalizing the high degree of conservation for the N-terminal residues of Tα and the contacting residues of UNC119. As expected for a hydrophobic environment, hydrogen-bonding potentials were satisfied by specific interactions. The first six peptide residues lack polar side chains, with the exception of S6, whose side chain is exposed to solvent. Most of the main chain groups participate in hydrogen bonds through the formation of a distorted 3_{10}-α helix by the first six residues of the peptide. Remaining buried polar groups of the peptide are coordinated by conserved UNC119 residues. The Y131 hydroxyl group hydrogen bonds with the lauroyl oxygen, E163 hydrogen bonds G2 NH, and Y220 coordinates A3 NH via a buried water molecule (**Fig. 4c**). This water molecule, along with E163 and Y220, constitute part of an extensive hydrogen-bonding network that also includes H165, H192, Y194, S218 and one other water molecule. These interactions provide specific recognition of N-terminal groups that define the location of the peptide-acyl junction in the UNC119 cavity, thereby establishing the length of acyl chain that can be accommodated. We also determined an isomorphous structure of UNC119 with the *C. elegans* ODR-3 lauroyl-GSCQSNENSE ligand (data not shown). This structure is superimposable with that of the Tα ligand, but with a

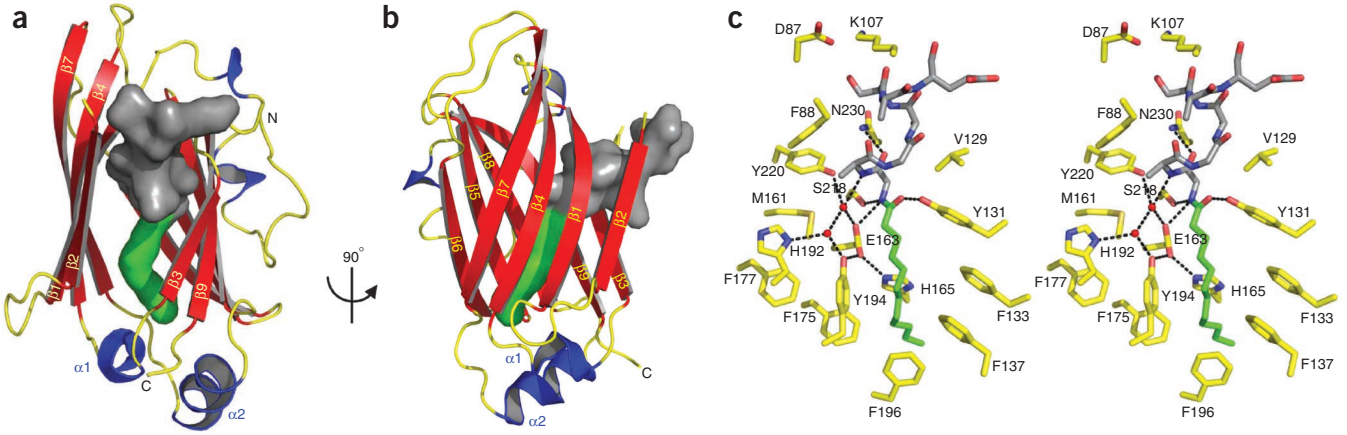

Figure 4 The lipid-binding pocket of UNC119. (**a**,**b**) Two orientations of UNC119 co-crystallized with the acylated Tα peptide in the UNC119 hydrophobic cavity. The lauroyl chain is shown in green and the ten amino acids of the peptide are modeled in dark gray. In **b**, UNC119 is viewed after a 90° rotation around the vertical axis and the individual β strands are labeled β1–9 in yellow. (**c**) Stereoview of UNC119 residues and key water molecules interacting with the lauroyl-GAGASAEEKH ligand. The hydrogen-bonding network (black dashed lines) limits the depth to which the Tα peptide can penetrate UNC119. Hydrogen bonds were included if the average of the bond length for all six molecules in the asymmetric unit was 3.2 Å or less and satisfied appropriate hydrogen bonding stereochemistry. UNC119 residues are shown in yellow, the lauroyl chain is green and the attached residues are colored dark gray. Figures were created with PyMOL (http://www.pymol.org/).

less-ordered peptide structure, consistent with the weaker binding affinity and absence of amino acid residues relevant for optimal binding.

GTP and UNC119 regulate transducin-membrane interactions

The co-crystal structure of UNC119 with the acylated Tα peptide implies that UNC119 may disrupt membrane association of Tα by binding the acyl chain into its hydrophobic pocket. To investigate whether UNC119 facilitates dissociation of transducin from membranes under isotonic conditions where it is firmly membrane associated, we examined the extraction of Tα by UNC119 in the presence and absence of GTP. Tα could be extracted from rod outer segments (ROS) membranes by UNC119 only in the presence of GTP (**Fig. 5a**), suggesting that GTP/GDP exchange and disruption of TαTβγ are essential for dissociation.

To demonstrate that UNC119 does not extract Tα-GDP–Tβγ from membranes, we investigated the interaction of UNC119 with Tα-GTP and Tα-GDP–Tβγ. *In vitro*, association of Tα-GDP–Tβγ to membranes can be disrupted in the dark by low salt (hypotonic) buffers in the absence of GTP[27]. In contrast, in the light, transducin is tightly bound to rhodopsin, requiring GDP/GTP exchange for disruption of the complex and membrane dissociation. Tα-GTP and Tα-GDP–Tβγ containing retinal lysates were prepared from light-adapted and dark-adapted retinas, respectively, and used for pulldown assays. Pulldowns indicated that UNC119 formed stable complexes with Tα-GTP (**Fig. 5b**), but not with Tα-GDP–Tβγ (**Fig. 5b**), confirming that disruption of Tα from Tα-GDP–Tβγ is necessary for the formation of the UNC119–Tα-GTP complex.

To determine whether UNC119 binding to Tα-GTP inhibits the GTPase activity of Tα, we measured GTP hydrolysis in a reconstituted system. Depleted ROS membranes containing rhodopsin exhibited very low GTPase activity originating from the remaining traces of transducin in the ROS membranes (**Fig. 5c**). The addition of transducin reconstituted GTPase activity, yielding a K_{cat} of 1.5 moles $GTP_{hydrolyzed}$ per mol of transducin per min. However, Tα-GTPase activity was nearly completely inhibited in the presence of recombinant UNC119. Collectively, these results indicate that neither GTP nor UNC119 alone were effective in solubilizing Tα from light-adapted membranes. The ability of UNC119 to extract Tα-GTP from membranes and stabilize GTP suggests that UNC119 may be important for the light-induced translocation of transducin (see Discussion).

UNC119 deletion in mouse affects transducin trafficking

The *Unc119*$^{-/-}$ mouse shows no obvious retinal degeneration early in life, but develops a slowly progressing photoreceptor degeneration beginning 6 months postnatally[12]. In the dark-adapted wild-type retina, Tα was detected almost exclusively in the outer segment (**Fig. 6a**), whereas in the dark-adapted *Unc119*$^{-/-}$ retina, Tα was partially retained in the inner segment and the outer nuclear layer (**Fig. 6b**). Transducin is thought to arrive at the outer segment by either vesicular transport[28] or passive diffusion[29], and UNC119 deletion appeared to have no effect on its localization.

A fascinating property of transducin is its observed translocation to the inner segment in-bulk during intense light exposure as part of a light-adaptation and desensitization mechanism. Under intense light, Tα-GTP and Tβγ translocate individually to the inner segment in minutes[30,31] by diffusion[32]. Both Tα and Tβγ return to the outer segments in hours during prolonged dark-adaptation[30], presumably by restricted diffusion[29], as transducin does return to outer segments in eyecups depleted of ATP, which is required for molecular motor-driven transport. To determine the effect of UNC119 deletion on the return of transducin by diffusion, we exposed wild-type and *Unc119*$^{-/-}$ mice to intense light for 60 min followed by prolonged dark-adaptation (0–24 h; **Fig. 6c**–**k**). Return of Tα was nearly complete in wild-type photoreceptors after 3 h of dark-adaptation, but a substantial amount of Tα remained associated with *Unc119*$^{-/-}$ inner segment membranes following prolonged dark-adaptation (**Fig. 6f**,**h**,**j**). The partial efficacy of UNC119 deletion on Tα mislocalization and the resulting slow degeneration may be attributable to redundant UNC119 isoforms (see Discussion).

ODR-3 and GPA-13 mistraffic in *unc-119* olfactory neurons

Originally discovered in *C. elegans*, *unc-119* mutants exhibit a complex phenotype, including defects in chemosensation, altered feeding behavior, inability to form dauer larvae[8] and excessive branching of motor neuron commissures[33]. We suspected G protein participation in polypeptide trafficking to olfactory cilia and investigated the

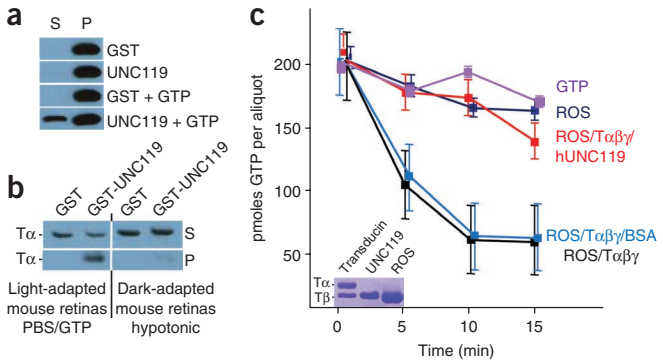

Figure 5 UNC119 interacts with Tα-GTP and inhibits GTPase activity. (**a**) Extraction of Tα from membranes by UNC119. Live mice were exposed to 10,000 lx over 20 min, driving transducin to the inner segments. Retina lysates in 1× phosphate-buffered saline (PBS) were incubated with either GST, mUNC119, GST and GTP, or mUNC119 and GTP, respectively. The soluble proteins (S) were separated from membrane-bound proteins (P) by centrifugation. Tα was detected by western blot using antibody to Tα. Tα elutes only in the presence of UNC119 and GTP. (**b**) Pulldown assays with light-adapted and dark-adapted mouse retinas. PBS/GTP supernatants from retinas of a light-adapted mouse (2,000 lx) and hypotonic supernatants from retinas of a dark-adapted mouse were used for pulldown assays, respectively. The proteins pulled down by GST or GST-UNC119 (pellet) and unbound proteins (supernatant) were analyzed by western blot using antibody to Tα. GST-UNC119 binds Tα-GTP (left), but not Tα-GDP–Tβγ (right). (**c**) GTPase activity of purified Tαβγ in the presence of ROS membranes. The activity of the reconstituted system (red line) corresponded to a rate of 1.5 mol GTP per min. Addition of bovine serum albumin (light blue) had little effect, whereas addition of UNC119 (green) reduced the activity nearly to baseline. Baseline activity was caused by a low amount of Tαβγ still attached to the membranes (see inset). Inset, SDS-PAGE of purified native transducin (only Tα and Tβ subunits are shown), recombinant human UNC119 and depleted ROS membranes containing rhodopsin and a trace of transducin (only Tα is visible, Tβ co-migrates with rhodopsin).

consequences of the *unc-119* deletion in *C. elegans* olfactory neurons. Although several G proteins participate in chemosensory signal transduction, ODR-3, predicted to be acylated at G2, is required to mediate signal transduction in AWA and AWC sensory neurons[34]. ODR-3 is localized predominantly to the cilia, with only trace amounts being found in the dendrites and cell bodies[35]. Immunolabeling of wild-type (**Fig. 7a** and **Supplementary Fig. 4a**) and *unc-119* mutant worms (**Fig. 7b** and **Supplementary Fig. 4b**) with antibody directed against ODR-3 revealed mislocalization of ODR-3 in the *unc-119* mutant worms. Correspondingly, although GPA-13 was present in the cilia of both wild-type (**Fig. 7c** and **Supplementary Fig. 4c**) and *unc-119* mutant (**Fig. 7d** and **Supplementary Fig. 4d**) ADF, ASH and AWC chemosensory neurons[35], it was downregulated and mislocalized in the mutant worm.

Reduced amounts of ODR-3 and GPA-13 present in the cilia of mutant worms could arise indirectly from abnormal neuronal morphology. To exclude this possibility, we crossed transgenic worms specifically expressing GFP in AWA, AWB or AWC neurons onto the *unc-119* mutant background. Ciliated endings of AWA and AWB neurons in *unc-119* mutants (**Supplementary Fig. 4f**,**h**) were identical to those in wild types (**Supplementary Fig. 4e**,**g**), but the shape of the AWC sensory ending in *unc-119* mutants (**Supplementary Fig. 4j**) was slightly different from that in wild types (**Supplementary Fig. 4i**). As the ciliary morphology of AWC neurons in the *unc-119* mutant was normal, however, it seems improbable that the decreased ODR-3 and GPA-13 protein levels observed in *unc-119* mutants were caused by disrupted cellular integrity.

To determine whether expression of transgenic, wild-type *unc-119* could restore G protein stability in amphid neurons, we introduced GFP::UNC-119 driven by the *gpa-13* promoter into *unc-119* mutant worms. GFP::UNC-119 expression was found in three pairs of amphid sensory neurons, presumably ADF, ASH and AWC (**Fig. 7**). Labeling with antibody to GPA-13 showed an increase in GPA-13 immunoreactivity in the cilia of the transgenic worms (**Fig. 7e**) relative to nontransgenic *unc-119* mutants (**Fig. 7f**). Because ODR-3 is also expressed in ADF, ASH and AWC neurons, transgenic worms were also labeled with antibody to ODR-3. Increased levels of ODR-3 were also detected in the cilia of transgenic worms (**Fig. 7g**) relative to nontransgenic *unc-119* mutant worms (**Fig. 7h**). Transgenic expression of supplemental UNC-119 in these neurons was capable of restoring the wild-type phenotype.

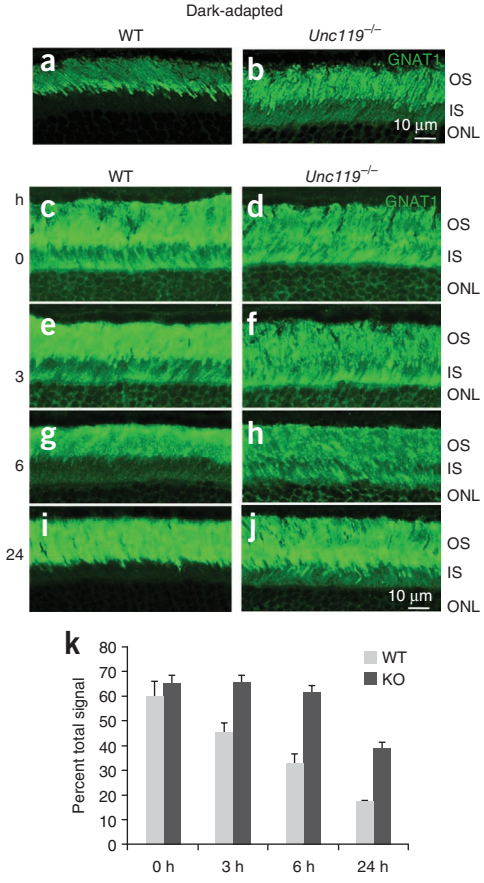

Figure 6 Slow return of transducin to the outer segment after intense light exposure. (**a**,**b**) Localization of Tα (green) in dark-adapted wild-type and *Unc119*$^{-/-}$ retina. Mice were dark-adapted for at least 12 h. Frozen sections were probed with antibody to Tα and FITC-linked secondary antibody. Note the presence of Tα in dark-adapted inner segments. (**c**–**j**) Mice were first exposed to intense light for 60 min, then dark-adapted for 3 h (**e**,**f**), 6 h (**g**,**h**) and 24 h (**i**,**j**). Frozen sections were probed with antibody to Tα and FITC-linked secondary antibody. Note that Tα slowly returned to the wild-type outer segment, but is blocked in part from returning to the *Unc119*$^{-/-}$ outer segment. IS, inner segment; ONL, outer nuclear layer; OS, outer segment. (**k**) Quantification of inner segment fluorescence at 0, 3, 6, and 24 h after start of dark-adaptation. Fluorescence signal was quantified using ImageJ software. Each bar included three independent measurements. Error bars denote means ± s.d.

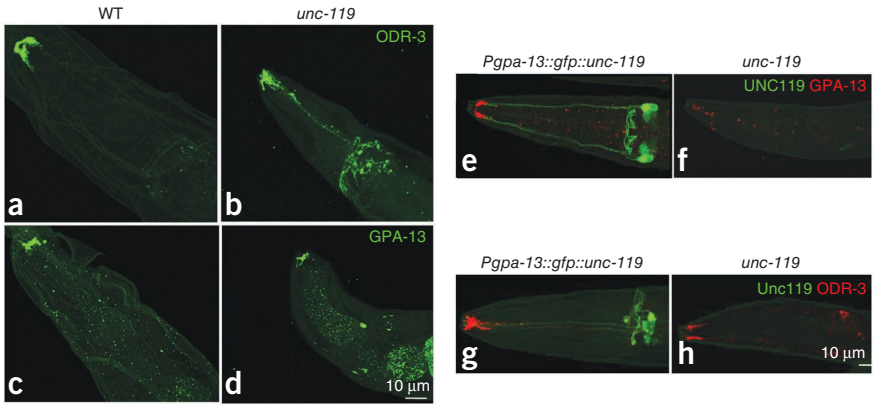

Figure 7 Mislocalization of the G proteins ODR-3 and GPA-13 in a *C. elegans unc-119(ed3)* mutant. (**a**–**d**) Wild-type (**a**,**c**) and *unc-119* mutant (**b**,**d**) *C. elegans* were stained with an antibody to ODR-3 (**a**,**b**) and GPA-13 (**c**,**d**). Mislocalization of ODR-3 and GPA-13 to the olfactory cell bodies and axons is evident in *unc-119* mutants. (**e**–**h**) Cell-specific rescue of *unc-119* in *C. elegans* restores GPA-13 and ODR-3 localization. The *unc-119* gene fused with GFP was driven by the *gpa-13* promoter in ADF, ASH and AWC in *unc-119* mutants. The transgenic (**e**,**g**) and *unc-119* mutant control (**f**,**h**) were labeled with GPA-13 (**e**,**f**) or ODR-3 antibodies (**g**,**h**).

DISCUSSION

The immunoglobulin β-sandwich fold demonstrated by the crystal structure of human UNC119 is similar to that seen in PrBP/δ (PDB ID: 1KSH)[23] and RhoGDI (PDB ID: 1DOA)[22]. PrBP/δ is a prenyl-binding protein and an important cofactor in the transport of prenylated proteins in photoreceptors[5]. RhoGDI extracts C-terminally geranylgeranylated Rac, Rho and CDC42 from membranes providing a hydrophobic environment for their prenyl anchors in its pocket, thereby trapping these small G proteins in their inactive GDP bound form[22]. The β strands of PrBP/δ and UNC119 align nicely when the two structures are superimposed (**Supplementary Fig. 2a**), whereas the β strands of RhoGDI and UNC119 are more divergent (**Supplementary Fig. 2b**). Important differences are seen in the UNC119 structure. The entrance through which the lipid enters the hydrophobic pocket in RhoGDI (and presumably PrBP/δ) is located at the opposite edge of the β-sandwich fold. The opening of the UNC119 pocket is completely occupied by the first six amino acids of Tα with the acyl chain deeply inserted into the cavity. These data, along with the extensive interactions that limit the depth to which the Tα peptide can penetrate the UNC119 cavity (**Fig. 4c** and **Supplementary Fig. 2a**,**b**), support the assertion that interaction specificity with lipidated proteins is based in part on the amino acid sequence immediately adjacent to the post-translational modification.

Unc119 and G protein trafficking

G protein subunits are either co-translationally acylated or acylated by an unidentified endoplasmic reticulum–resident acyl transferase. Acylated Gα and prenylated Gβγ most likely combine to form heterotrimeric G proteins at the endoplasmic reticulum[28]. Our results (**Fig. 6b**) indicate that the deletion of UNC119 in mouse leads to partial retention of transducin in the inner segment even after complete dark-adaptation, leaving post-biosynthesis transport largely intact. The partial effect seen in the *UNC119*$^{-/-}$ mouse is likely a result of the redundancy of UNC119 isoforms. UNC119B, encoded by the *UNC119B* gene located on human chromosome 5 (*UNC119* is on chromosome 17) is 61% similar and 52% identical to UNC119 and, similar to GST-UNC119, GST-UNC119B pulls down Tα from bovine retina lysate (R.C. and W.B., unpublished results).

In contrast with vertebrates, the *C. elegans* genome harbors only one UNC119 gene. Accordingly, *unc-119* null mutant phenotypes are more severe and UNC-119 deletion affects both neuronal and non-neuronal cells resulting in a complex phenotype. We focused on olfactory neurons, as defects in chemosensation have been reported in unc-119 knockout worms[8]. *C. elegans* relies on its 11 pairs of amphid neurons to detect odorants and soluble molecules[36]. These sensory neurons are polarized ciliated cells with an overall morphology similar to vertebrate photoreceptors. *unc-119* deletion in the worm results in the mislocalization and mistargeting of the G proteins ODR-3 and GPA-13, which are expressed in AWA, AWB, AWC, ASH and ADF amphid cells (**Fig. 7b**,**d**). Proper localization of ODR-3 and GPA-13 was restored by expressing transgenic UNC119 under the control of their intrinsic promoters (**Fig. 7e**,**g**). Notably, ODR-3, GPA-13 and Tα share only 27% overall sequence identity, with sequence similarity at the N-terminal 50 amino acids being very limited. The ODR-3 N-terminal peptide shares only three of ten amino acids with the Tα peptide (**Fig. 3c**), resulting in a lower affinity interaction with human UNC119, as shown by isothermal titration calorimetry (**Fig. 3b**).

Light-induced translocation of transducin by diffusion

Light-activation of rhodopsin triggers GTP/GDP exchange on Tα, causing Tα-GTP and Tβγ to dissociate and traffic to the inner segment by passive diffusion with a $t_{1/2}$ of 3–5 min for Tα and a $t_{1/2}$ of approximately 12 min for Tβγ[32]. Tβγ is known to associate with phosducin, which reduces its affinity for both Tα and rod outer segment membranes[37]. On return to the dark, both Tα and Tβγ subunits return to the outer segments in hours in wild-type mice. This same phenomenon has previously been described in eyecups depleted of ATP, without which molecular motors do not function[29]. Thus, a model in which 'restricted' diffusion is responsible for the return of Tα and Tβγ to the outer segments is plausible.

We propose that the restriction is provided by an enzymatically switchable sink in the inner segments. We determined that UNC119 elutes Tα bound to membranes only in the presence of GTP (**Fig. 5b**), suggesting that the dissociation of Tα-GTP and Tβγ is essential for UNC119/Tα-GTP complex formation. On arrival at the inner segment following light-induced translocation (**Supplementary Fig. 5a**), transducin subunits are presumed to recombine after Tα's intrinsic GTPase activity hydrolyzes GTP, permitting heterotrimeric transducin to dock to inner segment membranes, which are devoid of rhodopsin. In the absence of the guanine exchange factor rhodopsin (**Supplementary Fig. 5b**), GTP/GDP exchange is very slow (rate constant = 10^{-4} per s)[38]. Both the GTP requirement for Tα extraction from membranes and the slow rate constant suggest that this event is the rate-limiting step for return to the outer segment (**Supplementary Fig. 5b**). The rate constant dictates that it will take approximately 10^4 s (166 min) for transducin to return to the outer segment, which agrees with experimentally observed return rates[31,32]. On solubilization of the UNC119/Tα-GTP complex, it likely diffuses passively through the inner segment and connecting cilium, depositing Tα directly at discs in the outer segment. Following Tα-GTP solubilization, PrBP/δ may extract Tβγ, whose transport to the outer segment is severely affected in a PrBP/δ deletion model[5].

An alternate candidate for interaction with Tβγ is phosducin, deletion of which affects light-driven translocation of Tβγ to the inner segment[37]. The detection of UNC119 in the mouse photoreceptor sensory cilium complex[9] suggests a possible role for UNC119 in cargo assembly and intraflagellar transport, an argument that is further strengthened by the association of UNC119 with ARL3 and RP2 (retinitis pigmentosa protein 2), both of which localize to mouse and human cilia[9,15].

Our data provide evidence for UNC119 functioning as a lipid-binding protein as well as a necessary component in G protein trafficking. UNC119, along with G proteins, is distributed in virtually all living organisms from unicellular flagellated amoeba to mammals. Thus, our data in both mouse and *C. elegans* will likely prove helpful in elucidating mechanisms involved in membrane protein transport in the sensory systems of other species.

METHODS

Methods and any associated references are available in the online version of the paper at http://www.nature.com/natureneuroscience/.

Accession codes. Protein Data Bank: 3GQQ (UNC119) and 3RBQ (UNC119–lauroyl-GAGASAEEKH)

Note: Supplementary information is available on the Nature Neuroscience website.

ACKNOWLEDGMENTS

We thank R. Abramowitz and J. Schwanof for access to the X4A beamline at the National Synchrotron Light Source and G. DeTitta of Hauptman Woodward Research Institute for crystallization screening. This work was supported by US National Institutes of Health grants EY08123 (W.B.), EY019298 (W.B.), EY014800-039003 (National Eye Institute core grant), EY10848 (G.I.) and NS034307 (E.M.J.), by the Howard Hughes Medical Institute (E.M.J.), by a grant from the Protein Structure Initiative of the US National Institutes of Health (U54 GM074958), by the University of Utah Macromolecule Crystallography Core Facility, by a Center Grant of the Foundation Fighting Blindness to the University of Utah, and unrestricted grants to the Departments of Ophthalmology at the University of Utah from Research to Prevent Blindness. W.B. is a recipient of a Research to Prevent Blindness Senior Investigator Award.

AUTHOR CONTRIBUTIONS

H.Z. generated pulldown/light-induced translocation results and is responsible for *C. elegans* immunostaining and imaging. R.C. generated ITC results. R.C., F.G.W. and C.P.H. generated human UNC119/acylated Tα-peptide co-crystals and determined the structure. S.V., Y.C., J.S., Y.J.H., R.X., G.T.M. and L.T. determined the unbound human UNC119 structure. R.C., C.D.G. and W.B. isolated ROS membranes, transducin and determined GTPase activity. M.W.D. and E.M.J. generated transgenic *C. elegans* mutants. G.I. generated the Unc119 knockout mouse. H.Z., R.C., C.P.H., L.T. and W.B. wrote the manuscript.

COMPETING FINANCIAL INTERESTS

The authors declare no competing financial interests.

Published online at http://www.nature.com/natureneuroscience/.
Reprints and permissions information is available online at http://www.nature.com/reprints/index.html.

1. Rosenbaum, J.L. & Witman, G.B. Intraflagellar transport. *Nat. Rev. Mol. Cell Biol.* **3**, 813–825 (2002).
2. Jin, H. *et al.* The conserved Bardet-Biedl syndrome proteins assemble a coat that traffics membrane proteins to cilia. *Cell* **141**, 1208–1219 (2010).
3. Kim, J., Krishnaswami, S.R. & Gleeson, J.G. CEP290 interacts with the centriolar satellite component PCM-1 and is required for Rab8 localization to the primary cilium. *Hum. Mol. Genet.* **17**, 3796–3805 (2008).
4. Gillingham, A.K. & Munro, S. The small G proteins of the Arf family and their regulators. *Annu. Rev. Cell Dev. Biol.* **23**, 579–611 (2007).
5. Zhang, H. *et al.* Deletion of PrBPδ impedes transport of GRK1 and PDE6 catalytic subunits to photoreceptor outer segments. *Proc. Natl. Acad. Sci. USA* **104**, 8857–8862 (2007).
6. Keller, L.C. *et al.* Molecular architecture of the centriole proteome: the conserved WD40 domain protein POC1 is required for centriole duplication and length control. *Mol. Biol. Cell* **20**, 1150–1166 (2009).
7. Chung, S., Kang, S., Paik, S. & Lee, J. NgUNC-119, Naegleria homologue of UNC-119, localizes to the flagellar rootlet. *Gene* **389**, 45–51 (2007).
8. Maduro, M. & Pilgrim, D. Identification and cloning of unc-119, a gene expressed in the *Caenorhabditis elegans* nervous system. *Genetics* **141**, 977–988 (1995).
9. Liu, Q. *et al.* The proteome of the mouse photoreceptor sensory cilium complex. *Mol. Cell. Proteomics* **6**, 1299–1317 (2007).
10. Higashide, T., Murakami, A., McLaren, M.J. & Inana, G. Cloning of the cDNA for a novel photoreceptor protein. *J. Biol. Chem.* **271**, 1797–1804 (1996).
11. Swanson, D.A., Chang, J.T., Campochiaro, P.A., Zack, D.J. & Valle, D. Mammalian orthologs of *C. elegans* unc-119 highly expressed in photoreceptors. *Invest. Ophthalmol. Vis. Sci.* **39**, 2085–2094 (1998).
12. Ishiba, Y. *et al.* Targeted inactivation of synaptic HRG4 (UNC119) causes dysfunction in the distal photoreceptor and slow retinal degeneration, revealing a new function. *Exp. Eye Res.* **84**, 473–485 (2007).
13. Higashide, T., McLaren, M.J. & Inana, G. Localization of HRG4, a photoreceptor protein homologous to Unc-119, in ribbon synapse. *Invest. Ophthalmol. Vis. Sci.* **39**, 690–698 (1998).
14. Kobayashi, A., Kubota, S., Mori, N., McLaren, M.J. & Inana, G. Photoreceptor synaptic protein HRG4 (UNC119) interacts with ARL2 via a putative conserved domain. *FEBS Lett.* **534**, 26–32 (2003).
15. Veltel, S., Kravchenko, A., Ismail, S. & Wittinghofer, A. Specificity of Arl2/Arl3 signaling is mediated by a ternary Arl3-effector-GAP complex. *FEBS Lett.* **582**, 2501–2507 (2008).
16. Haeseleer, F. Interaction and colocalization of CaBP4 and Unc119 (MRG4) in photoreceptors. *Invest. Ophthalmol. Vis. Sci.* **49**, 2366–2375 (2008).
17. Alpadi, K. *et al.* RIBEYE recruits Munc119, a mammalian ortholog of the *Caenorhabditis elegans* protein unc119, to synaptic ribbons of photoreceptor synapses. *J. Biol. Chem.* **283**, 26461–26467 (2008).
18. Kobayashi, A. *et al.* HRG4 (UNC119) mutation found in cone-rod dystrophy causes retinal degeneration in a transgenic model. *Invest. Ophthalmol. Vis. Sci.* **41**, 3268–3277 (2000).
19. Vepachedu, R., Karim, Z., Patel, O., Goplen, N. & Alam, R. Unc119 protects from Shigella infection by inhibiting the Abl family kinases. *PLoS ONE* **4**, e5211 (2009).
20. Gorska, M.M., Cen, O., Liang, Q., Stafford, S.J. & Alam, R. Differential regulation of interleukin 5–stimulated signaling pathways by dynamin. *J. Biol. Chem.* **281**, 14429–14439 (2006).
21. Bork, P., Holm, L. & Sander, C. The immunoglobulin fold. Structural classification, sequence patterns and common core. *J. Mol. Biol.* **242**, 309–320 (1994).
22. Hoffman, G.R., Nassar, N. & Cerione, R.A. Structure of the Rho family GTP-binding protein Cdc42 in complex with the multifunctional regulator RhoGDI. *Cell* **100**, 345–356 (2000).
23. Hanzal-Bayer, M., Renault, L., Roversi, P., Wittinghofer, A. & Hillig, R.C. The complex of Arl2-GTP and PDE delta: from structure to function. *EMBO J.* **21**, 2095–2106 (2002).
24. Zhang, H. *et al.* Photoreceptor cGMP phosphodiesterase delta subunit (PDEdelta) functions as a prenyl-binding protein. *J. Biol. Chem.* **279**, 407–413 (2004).
25. Goc, A. *et al.* Different properties of the native and reconstituted heterotrimeric G protein transducin. *Biochemistry* **47**, 12409–12419 (2008).
26. Kerov, V. *et al.* N-terminal fatty acylation of transducin profoundly influences its localization and the kinetics of photoresponse in rods. *J. Neurosci.* **27**, 10270–10277 (2007).
27. Baehr, W., Morita, E., Swanson, R. & Applebury, M.L. Characterization of bovine rod outer segment G protein. *J. Biol. Chem.* **257**, 6452–6460 (1982).
28. Marrari, Y., Crouthamel, M., Irannejad, R. & Wedegaertner, P.B. Assembly and trafficking of heterotrimeric G proteins. *Biochemistry* **46**, 7665–7677 (2007).
29. Slepak, V.Z. & Hurley, J.B. Mechanism of light-induced translocation of arrestin and transducin in photoreceptors: interaction-restricted diffusion. *IUBMB Life* **60**, 2–9 (2008).
30. Sokolov, M. *et al.* Massive light-driven translocation of transducin between the two major compartments of rod cells: a novel mechanism of light adaptation. *Neuron* **34**, 95–106 (2002).
31. Elias, R.V., Sezate, S.S., Cao, W. & McGinnis, J.F. Temporal kinetics of the light/dark translocation and compartmentation of arrestin and alpha-transducin in mouse photoreceptor cells. *Mol. Vis.* **10**, 672–681 (2004).
32. Calvert, P.D., Strissel, K.J., Schiesser, W.E., Pugh, E.N. Jr. & Arshavsky, V.Y. Light-driven translocation of signaling proteins in vertebrate photoreceptors. *Trends Cell Biol.* **16**, 560–568 (2006).
33. Knobel, K.M., Davis, W.S., Jorgensen, E.M. & Bastiani, M.J. UNC-119 suppresses axon branching in *C. elegans*. *Development* **128**, 4079–4092 (2001).
34. Roayaie, K., Crump, J.G., Sagasti, A. & Bargmann, C.I. The G alpha protein ODR-3 mediates olfactory and nociceptive function and controls cilium morphogenesis in *C. elegans* olfactory neurons. *Neuron* **20**, 55–67 (1998).
35. Lans, H., Rademakers, S. & Jansen, G. A network of stimulatory and inhibitory Galpha-subunits regulates olfaction in *Caenorhabditis elegans*. *Genetics* **167**, 1677–1687 (2004).
36. Perkins, L.A., Hedgecock, E.M., Thomson, J.N. & Culotti, J.G. Mutant sensory cilia in the nematode *Caenorhabditis elegans*. *Dev. Biol.* **117**, 456–487 (1986).
37. Sokolov, M. *et al.* Phosducin facilitates light-driven transducin translocation in rod photoreceptors. Evidence from the phosducin knockout mouse. *J. Biol. Chem.* **279**, 19149–19156 (2004).
38. Cowan, C.W., Wensel, T.G. & Arshavsky, V.Y. Enzymology of GTPase acceleration in phototransduction. *Methods Enzymol.* **315**, 524–538 (2000).

ONLINE METHODS

Animals. Mice were maintained in a 12:12 h dark-light cycle. The animals' care was approved by the Institutional Animal Care and Use Committee of the University of Utah. To dark-adapt, we placed the mice in the dark for 12 h or more. For light-adaptation, the pupils of the mice were dilated with 1% tropicamine (wt/vol) and the mice were illuminated by 2,000 lx for 60 min. Following light-adaptation, mice were returned to the dark for 3, 6 or 24 h. *Unc119*$^{-/-}$ mice were from the colony of G.I.[12]. *Gnat1*$^{-/-}$ animals were obtained from J. Lem (Tufts University).

***C. elegans* strains.** Strains were maintained using standard methods. Strains were obtained from Caenorhabditis Genetics Center, M. Maduro (University of California, Riverside) and P. Sengupta (Brandeis University). Stably integrated strains used in this work were *oyIs[P(odr-10)::gfp] V* for examining AWA neurons, *lin-15(n765ts) X kyIs104[str-1::GFP, lin-15(+)] X* for examining AWB neurons[39], and *kyIs140[str-2::GFP + lin-15(+)]* for examining AWC neurons[39]. The AWA, AWB, and AWC neurons expressing the above stably integrated GFP markers were also examined in *unc-119(ed3)* mutants. Double mutant strains were generated using standard methods.

Crystallization of UNC119. Expression and purification of truncated human UNC119 protein (residues 56–240) was carried out as a part of the established high-throughput protein production pipeline[40] (Northeast Structural Genomics Consortium target HR3066a). The protein was cloned into the pET 14-15C expression vector (Novagen). Selenomethionyl protein was expressed in *Escherichia coli* BL21(DE3) + Magic, and purified using Ni-NTA affinity chromatography (Qiagen) and gel filtration (Superdex 75, Amersham/GE Healthcare) in buffer containing 10 mM TrisHCl, 100 mM NaCl, 5 mM DTT, pH 7.5. Protein homogeneity was verified by SDS-PAGE and MALDI-TOF mass spectrometry.

Preliminary crystallization trials were performed using the microbatch crystallization under paraffin oil at 4 °C[41]. UNC119 crystals useful for structure determination were grown in a 1:1 ratio with solution containing 40% PEG 4000 (wt/vol), 0.1 M potassium acetate, 0.1 M sodium acetate, pH 5.0 at 4 °C. The crystals grew to 0.025, 0.05, 0.1 mm after 3–4 weeks and were transferred to paratone oil and frozen in liquid propane. Single crystals were maintained at 100 K and used to collect a SAD dataset at beamline X4A at the National Synchrotron Light Source using an ADSC Quantum-4 CCD detector. Data were integrated and scaled using the HKL2000 package[42].

SHELXE/D[43] was used to locate selenium sites and calculate initial phases. Solvent flattening and partial model building were performed using RESOLVE[44]. The remainder of the model was built manually using COOT[45] and was refined with PHENIX[46]. Data collection and refinement statistics are presented in **Supplementary Table 1**. The quality of the model was checked using MolProbity[47]. The atomic coordinates and structure factors for UNC119 (PDB ID: 3GQQ) have been deposited in the Protein Data Bank.

UNC119/lauroyl-GAGASAEEKH crystal growth and data collection. UNC119 (**Supplementary Table 1**) was co-crystallized with a Tα peptide (lauroyl-GAGASAEEKH). Purified UNC119 and the Tα peptide were dissolved in 10 mM Tris pH 7.4, 100 mM NaCl and 5 mM DTT. The protein solution was prepared by mixing purified UNC119 and the Tα peptide (1:1.1 molar ratio) for at least 1 h at 4 °C. Crystals were grown in drops containing 3 µl UNC119 Tα peptide mixture and 3 µl 40% PEG 5000 (wt/vol), 0.1 M sodium acetate, 0.1 M potassium acetate, pH 5.0 and 1.8 µl 30% isopropanol (vol/vol) at 4 °C, under 40 µl paraffin oil. Crystals were harvested for data collection after 10–14 d.

Crystals were mounted in a nylon loop, briefly immersed in cryoprotection buffer (40% PEG 5000, 0.1 M sodium acetate, 0.1 M potassium acetate, 12% glycerol (vol/vol), pH 5.0) and cooled by plunging into liquid nitrogen. Crystals were maintained at 100 K during data collection. Data were collected at beam line BL9-2 of the Stanford Synchrotron Radiation Lightsource. Data were integrated and scaled using DENZO and SCALEPACK, respectively[42]. Data were phased by molecular replacement using PHASER[48] using PDB code 3GQQ as the search model. The models were rebuilt using O[49] and refined against a maximum likelihood target function using REFMAC[50]. Structures were checked using MolProbity[47].

Expression and purification of recombinant bovine UNC119 protein. The *UNC119* cDNA was amplified by PCR from a bovine retina cDNA library and cloned into the BamHI/EcoRI sites of a pGEX-2T vector (Amersham/GE Healthcare). A His-tag (6 histidines) was placed immediately following the ATG of the *UNC119* cDNA. The construct was transformed into the *E. coli* expression strain ER2556 (New England Biolab). Expression of the recombinant protein was induced by 0.1 mM IPTG for 5 h at 37 °C. The protein was purified by a Histrap (Amersham/GE Healthcare) column followed by a GSTrap column (Amersham/GE Healthcare) according to the manufacturer's protocol and reduced glutathione was removed by a Microcon centrifuge filter with an exclusion size of 30 kDa (Millipore).

Expression and purification of recombinant human UNC119. *Unc119* cDNA was amplified by PCR from a human retina cDNA library and directionally cloned into a pET151/D-TOPO vector (Invitrogen). The 6× His-tag in the vector was converted to a 12× His-tag using a QuickChange site-directed mutagenesis kit (Stratagene) and verified by DNA sequencing. The construct was expressed in BL21 Codon+ *E. coli* cells (Stratagene) in ZY autoinduction media for 6 h at 37 °C and then overnight at 19 °C. Cells were harvested by centrifugation, resuspended, and lysed in 10 mg ml^{-1} lysozyme in lysis buffer (20 mM imidazole, 700 mM NaCl, 50 mM Tris pH 7.4, 1 mM DTT) and protease inhibitors (PMSF, aprotinin, leupeptin, pepstatin) for 1 h at 4 °C, followed by sonication. The lysate was clarified by centrifugation (45 min, 20,000*g*) and soluble hUNC119 protein was bound to a Ni^{2+} sepharose column (Amersham/GE Healthcare), washed with ten column volumes of lysis buffer and eluted with 300 mM imidazole in 700 mM NaCl, 50 mM Tris pH 7.4, and 1 mM DTT. Fractions were assayed by SDS-PAGE, pooled, and the 12× His-tag was removed by incubation with TEV protease (~1 mg per 100 mg protein, 20 h at 25 °C) in 2l of 500 mM NaCl, 50 mM Tris pH 7.4, and 1 mM DTT. Unprocessed protein and TEV were removed by Ni^{2+} sepharose chromatography, cleaved protein was collected in the flow through, concentrated, and purified to homogeneity by anion exchange (HiTrap Q FF, GE Life Sciences, 20–1,000 mM NaCl gradient in 25 mM Tris pH 7.4, 1 mM DTT) and gel filtration (SD200, Amersham/GE Healthcare; 100 mM NaCl, 25 mM Tris pH 7.4, 1 mM DTT) chromatography.

Pulldown assays. For protein sequencing, a bovine retina was homogenized by brief sonication in 1 ml PBS buffer (137 mM NaCl, 2.7 mM KCl, 10 mM Na_2HPO_4. 1.76 mM KH_2PO_4 pH 7.4) with 1 mM DTT and protease inhibitor cocktail (Roche). The insoluble debris was removed by centrifugation. The retina lysate was mixed with 10–80 µg of purified GST-UNC119 or 40 µg of GST followed by overnight incubation at 4 °C. GST-UNC119 and its interacting proteins were pulled down by glutathione beads and the bound proteins were eluted with SDS gel-loading buffer. The proteins were resolved by 12.5% SDS-PAGE. The protein sequencing by LC-MS/MS was carried out in the Mass Spectrometry Core Facility at the University of Utah.

For the competitive binding assay (**Fig. 3a**), 400 µl of retina lysate was incubated with 10 µg GST-UNC119 in the presence of 150 µg lauroyl-GAGASAEEKH and GAGASAEEKH peptides, respectively. All peptides were synthesized by the Utah Peptide Core facility.

For pulldowns with light- and dark-adapted retinas, mouse retinas were homogenized in 1× PBS buffer containing 40 µM GTP (light) or hypotonic buffer (dark) (10 mM TrisHCl pH 7.4, 1 mM EDTA, 0.1 mM DTT). The insoluble fraction was removed by centrifugation. The supernatant was used for pulldown assays using GST and GST-UNC119. Solubilized transducin was reconstituted in 1× PBS buffer, pulled down with GST-UNC119 and identified by western blot using antibody to Tα (UUTA).

Immunoblot. Proteins were separated by 12.5% (for detection of Tα and GCAP1) or 15% (for detection of Tα and Tγ) SDS-PAGE and transferred to a nitrocellulose membrane. Membranes were processed as described[24]. The dilutions of the primary antibodies were 1:10,000 for SC389 (antibody to rod Tα, Santa Cruz Biotechnology), 1:6,000 UW101 (antibody to GCAP1), 1:10,000 for UUTA (antibody to rod Tα) and 1:5,000 for GN2 (antibody to rod Tγ). UUTA and GN2 were obtained from C.K. Chen (Virginia Commonwealth University).

Extraction of transducin from mouse retinal membrane by UNC119. Mouse retinas were prepared from wild-type mice undergoing 20 min light-adaptation followed by 30 min dark-adaptation. The retinas were homogenized in 200 µl PBS with 1 mM DTT and protease inhibitors. The soluble components were removed by centrifugation at 4 °C for 10 min. The pellet was washed once with PBS, resuspended in 400 µl PBS, and aliquoted in four microcentrifuge tubes.

doi:10.1038/nn.2835

In these four tubes, 9 μg GST, 9 μg GST and 40 μM GTP (final concentration), 18 μg GST-UNC119, and 18 μg GST-UNC119 and 40 μM GTP (final concentration) were added, respectively. After overnight incubation at 4 °C, the membrane was pelleted and the supernatant was removed. The pellet was resuspended in 100 μl PBS. 10 μl of the supernatant from each tubes and their corresponding pellets were subjected to western blot using antibody to Tα (UUTA).

***In vitro* expression of Tα and Tα(G2A).** *Gnat1* cDNA was amplified from a bovine cDNA library and cloned into the XhoI and NotI sites of pEGFP-N2 vector to replace the eGFP gene. The G2A mutant construct was generated by site-directed mutagenesis kit (Stratagene). Hek293 cells were transfected using Lipofectamine 2000 (Invitrogen) following the manufacturer's instructions. The cells were harvested 48 h after transfection.

Immunocytochemistry of retina sections. Immunocytochemistry was performed as described[5]. Dilutions for the primary antibodies were 1:1,000 for UUTA (antibody to rod Tα) and 1:1,000 for G8 (antibody to GRK1). FITC-conjugated secondary antibodies were diluted 1:300.

ITC. The transducin N-terminal peptides lauroyl-, myristoyl-GAGASAEEKH or GAGASAEEKH, and recombinant human UNC119 protein samples were suspended in 25 mM Tris (pH 7.4), 100 mM NaCl and 1 mM DTT. Peptide and hUNC119 concentrations were varied as a result of the varying solubility of the peptides in the above-described buffer. ITC measurements were done on a MicroCal ITC-200 MicroCalorimeter at 25 °C. The peptide was injected into the hUNC119 samples at 180-s intervals. Data obtained from the peptide injections into the buffer blanks were subtracted from the experimental data for analysis using the MicroCal Origin Software.

GTPase assay. Transducin and depleted ROS membranes were purified from bovine retinas as previously described[27].The GTPase assay mix (20 μl) contained 4 pmoles (0.17 μg) rhodopsin (in depleted ROS membranes), 54 pmoles transducin (4.5 μg), 61 μM GTP spiked with γ-P^{32}-GTP, 20 mM Tris HCl pH 7.5, 5 mM $MgCl_2$, 1 mM DTT and 0.1 mM EDTA. Some assays included 133 pmoles UNC119 (2.27 μg) or 130 pmoles of BSA. Assays were incubated at 35 °C, 2 μl aliquots were withdrawn at 0, 5, 10, 15 and 20 min and spotted on PEI cellulose (Brinkmann). The PEI plates were washed in 0.12 M LiCl (30 min) and quantitated using a Typhoon Trio (GE Health Sciences) and Image Quant software.

Immunocytochemistry of *C. elegans*. Animals were permeabilized, fixed and stained following standard methods. The images were acquired using an FV1000 Olympus confocal microscope. Polyclonal ODR-3 and GPA-13 antibodies were gifts from G. Jansen (Center for Biomedical Genetics).

Cell-specific rescue of *C. elegans unc-119* mutant. The DNA used for microinjection was generated by fusion PCR. Briefly, the GFP gene was amplified by PCR from pPD104.53 (provided by A. Fire, Stanford) and cloned into P#MM016, in which the GFP cDNA was fused in frame to the 5′ of *unc-119* genomic DNA. The *gfp-unc119* fusion gene including the flanking transcription termination sequence was amplified by PCR. A 2.7-kb promoter sequence of *gpa-13* was amplified from *C. elegans* genomic DNA. The 3′ end of the *gpa-13* promoter was fused to the 5′ end of the *gfp-unc119* fusion gene by nested-PCR. The PCR product from the fusion PCR was microinjected into the germline.

39. Troemel, E.R., Kimmel, B.E. & Bargmann, C.I. Reprogramming chemotaxis responses: sensory neurons define olfactory preferences in *C. elegans*. *Cell* **91**, 161–169 (1997).
40. Acton, T.B. *et al*. Robotic cloning and Protein Production Platform of the Northeast Structural Genomics Consortium. *Methods Enzymol.* **394**, 210–243 (2005).
41. Chayen, N.E., Stewart, P.D., Maeder, D.L. & Blow, D.M. An automated system for micro-batch protein crystallization and screening. *J. Appl. Crystallogr.* **23**, 297–302 (1990).
42. Otwinowski, Z. & Minor, D. Processing of X-ray diffraction data collected in oscillation mode. *Methods Enzymol.* **276**, 307–326 (1997).
43. Schneider, T.R. & Sheldrick, G.M. Substructure solution with SHELXD. *Acta Crystallogr. D Biol. Crystallogr.* **58**, 1772–1779 (2002).
44. Terwilliger, T.C. SOLVE and RESOLVE: automated structure solution and density modification. *Methods Enzymol.* **374**, 22–37 (2003).
45. Emsley, P. & Cowtan, K. Coot: model-building tools for molecular graphics. *Acta Crystallogr. D Biol. Crystallogr.* **60**, 2126–2132 (2004).
46. Adams, P.D. *et al.* PHENIX: building new software for automated crystallographic structure determination. *Acta Crystallogr. D Biol. Crystallogr.* **58**, 1948–1954 (2002).
47. Davis, I.W. *et al*. MolProbity: all-atom contacts and structure validation for proteins and nucleic acids. *Nucleic Acids Res.* **35**, W375–383 (2007).
48. McCoy, A.J. *et al*. Phaser crystallographic software. *J. Appl. Crystallogr.* **40**, 658–674 (2007).
49. Jones, T.A., Zou, J.Y., Cowan, S.W. & Kjeldgaard, M. Improved methods for building protein models in electron density maps and the location of errors in these models. *Acta Crystallogr. A* **47**, 110–119 (1991).
50. Murshudov, G.N., Vagin, A.A. & Dodson, E.J. Refinement of macromolecular structures by the maximum-likelihood method. *Acta Crystallogr. D Biol. Crystallogr.* **53**, 240–255 (1997).

SUPPLEMENTAL MATERIAL

UNC119 is required for G protein trafficking in sensory neurons

Houbin Zhang, Ryan N. Constantine, Sergey Vorobiev, Yang Chen, Jayaraman Seetharaman, Yuanpeng Janet Huang, Rong Xiao, Gaetano T. Montelione, Cecilia D. Gerstner, M. Wayne Davis, George Inana, Frank G. Whitby, Erik M. Jorgensen, Christopher P. Hill, Liang Tong, and Wolfgang Baehr

Inventory

Table S1: UNC119 crystallographic data and refinement statistics

Data		
Crystal	HR3066a[a]	Au10pe
Space Group	$P2_12_12_1$	$P2_12_12_1$
Unit Cell Dimensions	a=77.89, b= 79.56, c=189.72	a=78.55, b=79.71 , c=189.59
Resolution (Å)	50.0 – 1.95	30.0 – 2.00
Resolution (Å) (high-resolution shell)	(2.02 – 1.95)	(2.07 – 2.00)
# Reflections measured	1,169,802	1,252,665
# Unique reflections	166,290[a]	82,342
Redundancy	7.0	15.2
Completeness (%)	99.6 (100)	100 (100)
$<I/\sigma(I)>$	26 (2.9)	11 (2.5)
Mosaicity (^{o})	0.37	1.1
Rsym[b]	0.088 (0.537)	0.116 (0.701)
Refinement		
Resolution (Å)	40.51 – 1.95	29.37 – 1.99
Resolution (Å) – (high-resolution shell)	(1.97 – 1.95)	(2.04 – 1.99)
# Reflections used for refinement	165,606[a]	78,089
# Reflections in Rfree set (%)	8,332 (5.0)	4,139 (5.3)
R[c]	0.191 (0.247)	0.200 (0.226)
Rfree[d]	0.214 (0.251)	0.250 (0.276)
RMSD: bonds (Å) / angles (°)	0.005 / 1.3	0.012 / 1.304
<B> (Å^2): Tα peptide residues/ # atoms	N/A	41 / 268
<B> (Å^2): UNC119 only / # atoms	33 / 8,265	29 / 8,299
<B> (Å^2): water molecules / # water	41 / 803	39 / 793
ϕ/ψ most favored (%)	99	97

Values in parenthesis refer to data in the high resolution shell.

[a] Friedel pairs were used in phasing and refining HR3066a.

[b] Rsym = $\Sigma|I-<I>|/\Sigma I$ where I is the intensity of an individual measurement and <I> is the corresponding mean value.

[c] R = $\Sigma||Fo|-|Fc||/\Sigma|Fo|$, where $|Fo|$ is the observed and $|Fc|$ the calculated structure factor amplitude.

[d] Rfree is the same as R calculated with a randomly selected test set of 5% (HR3066a[a]) or 5.3% (Au10pe) reflections that were never used in refinement calculations.

Table S2. Comparison of the RMSD values for each of the six UNC119 chains and their associated ligands.

Structures were overlapped on the UNC119 protein carbon-α atoms only. Ligand atoms were not included in the overlap calculation. RMSD values are given for the overlap of all protein atoms in each chain, all atoms related to residue 501 (glycine and the attached lauroyl group), and the carbon-α trace for the peptide attached to the lauroyl group in each ligand.

Chains Overlapped	RMSD for all protein atoms	RMSD for residue 501[a]	RMSD of Cα trace[b]
B on A	0.373	0.252	0.190 (501-507)
C on A	0.459	0.315	0.180 (501-504)
D on A	0.320	0.284	0.182 (501-504)
E on A	0.449	0.370	0.323 (501-503)
F on A	0.458	0.635	0.424 (501-507)

[a]RMSD values calculated using all atoms on residue 501 with residue 501 defined as glycine plus the attached lauroyl group.

[b]Numbers in parentheses refer to residues on the ligand from which the RMSD values were calculated.

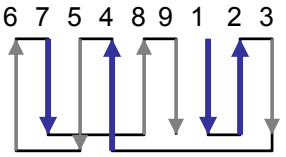

Figure S1A The Greek Key Motif in UNC119, RhoGDI and PrBP/δ (related to Fig. 1). Greek key motif of the β-sandwich fold common to the three structures. Blue arrows depict the strands that form one β-sheet, while gray arrows depict strands of the second β-sheet.

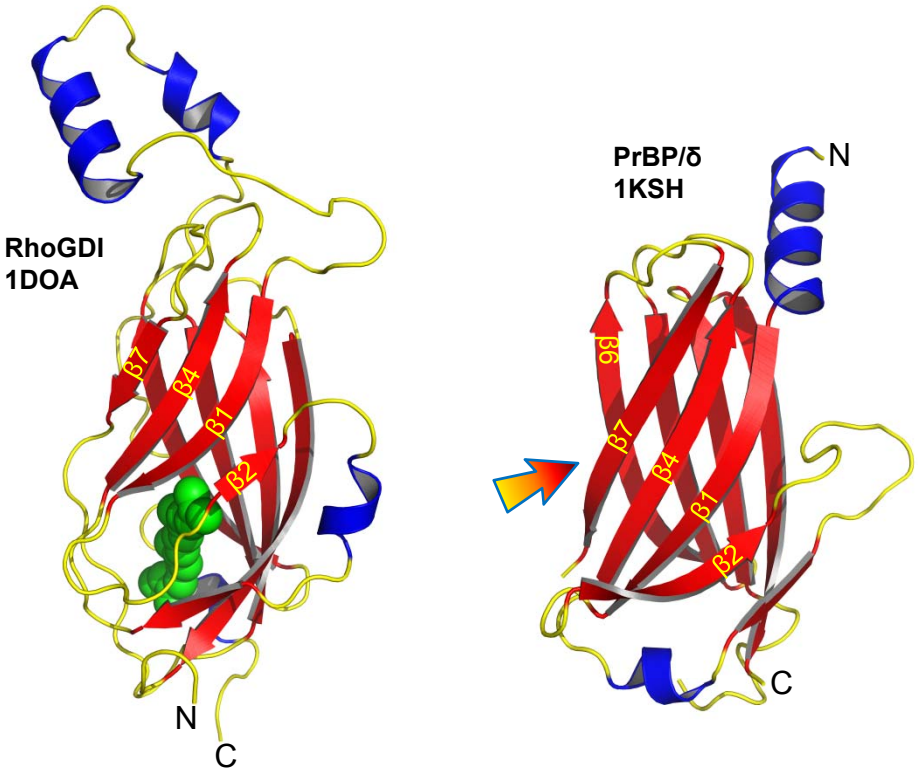

Figure S1B Ribbon representation of the geranylgeranyl binding protein RhoGDI (1DOA) and the prenyl binding protein PrBP/δ (1KSH). RhoGDI is shown with Cys-geranylgeranyl of CDC42 present in its binding pocket. The presumed entrance to the hydrophobic pocket of PrBP/δ is indicated with an arrow. Note that entrances to the hydrophobic pocket in UNC119 (Fig. 4A,B) and RhoGDI are located at the opposite edge of the β-sandwich fold. Figure created with PyMOL (www.pymol.org).

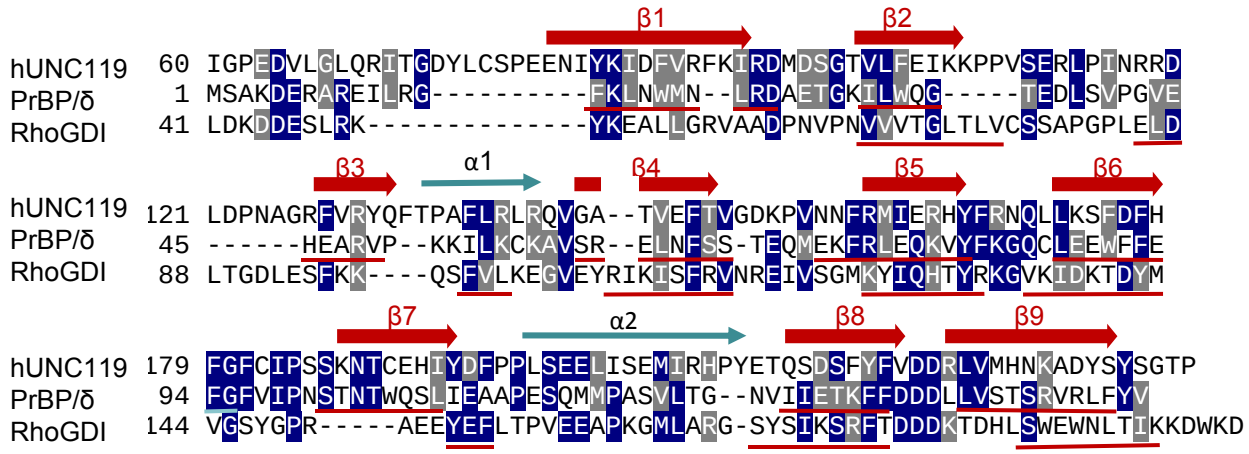

Figure S1C Sequence Alignment of Human UNC119, PrBP/δ, and RhoGDI. Only C-terminal residues of UNC119 (60-240) and RhoGDI (41-204) are shown. β-strands are depicted as large red arrows for UNC119 and are underlined in red for PrBP/δ and RhoGDI. Identical residues are highlighted blue and similar residues gray.

Nature Neuroscience: doi:10.1038/nn.2835

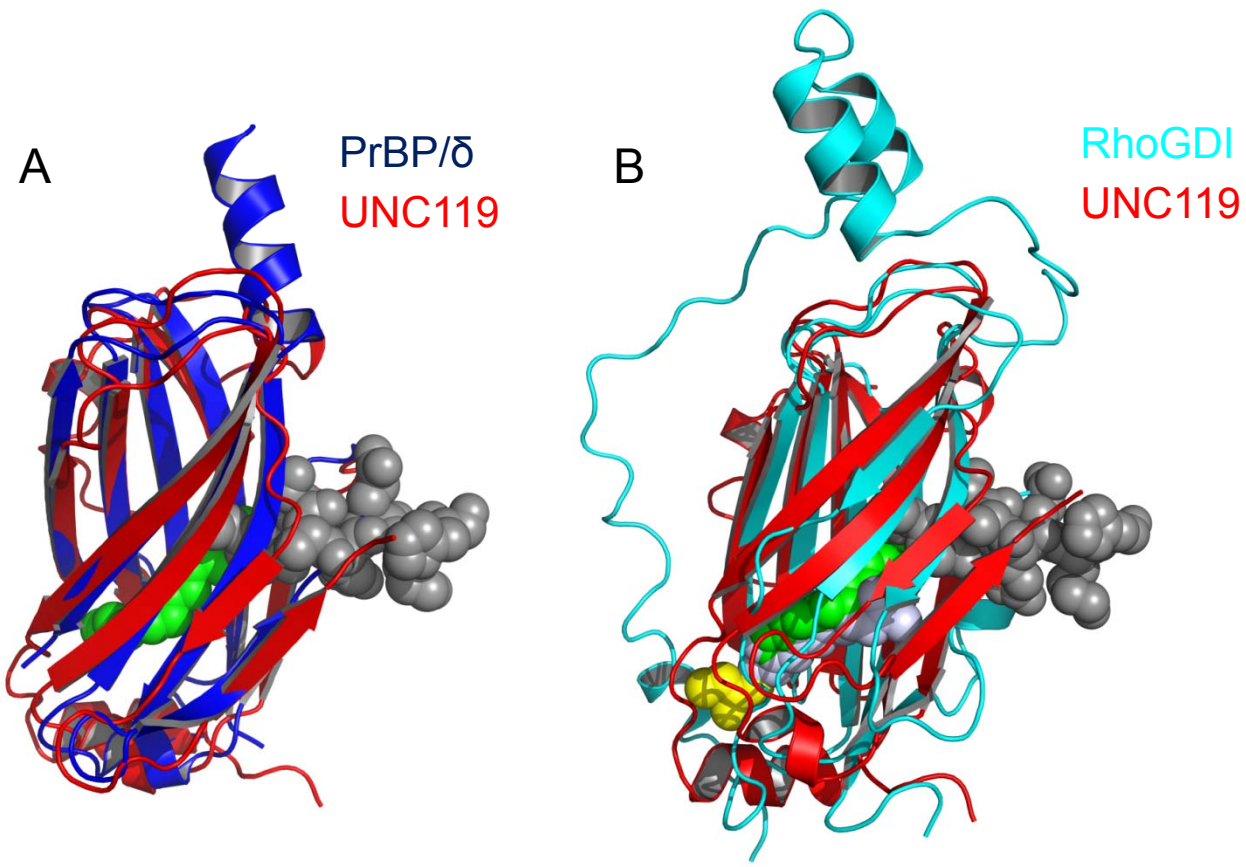

Figure S2A,B Structural Alignment of UNC119 with PrBP/δ and RhoGDI (related to Figure 4). (**A**) UNC119 (red) (PDB 3RBQ) aligned with PrBP/δ (blue). The Tα peptide is shown in dark gray and the acyl chain in green. Figure created with PyMOL (www.pymol.org). (**B**) UNC119 (red) aligned with RhoGDI (cyan). The Tα peptide is shown in dark gray and the acyl chain in green. The geranylgeranyl chain of the GTPase CDC42 bound to RhoGDI is shown in light gray. Figures created with PyMOL (www.pymol.org).

Fig. S2C
Zhang et al.

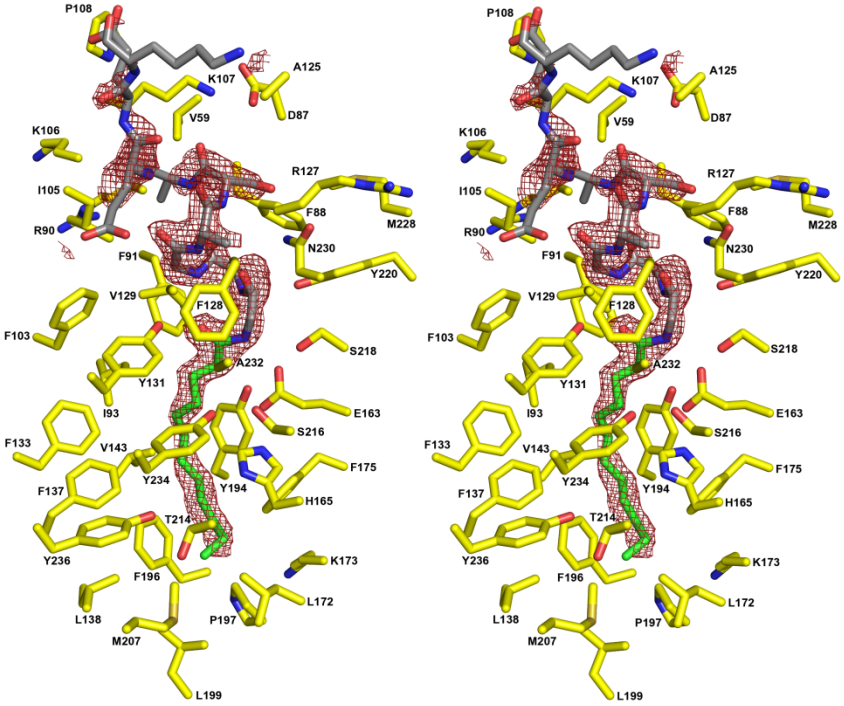

Figure S2C Electron density surrounding the Lauroyl-Tα peptide. A stereoview showing a simulated annealing Fo-Fc omit map contoured at 2.5 sigma (red mesh). Phases were calculated following deletion of the ligand, application of random shifts (0.1 A), and refinement of the resulting model. UNC119 residues that comprise the walls of the cavity are shown with yellow carbon atoms, the acyl chain is colored green, and residues that comprise the remainder of the Tα peptide are colored gray.

Nature Neuroscience: doi:10.1038/nn.2835

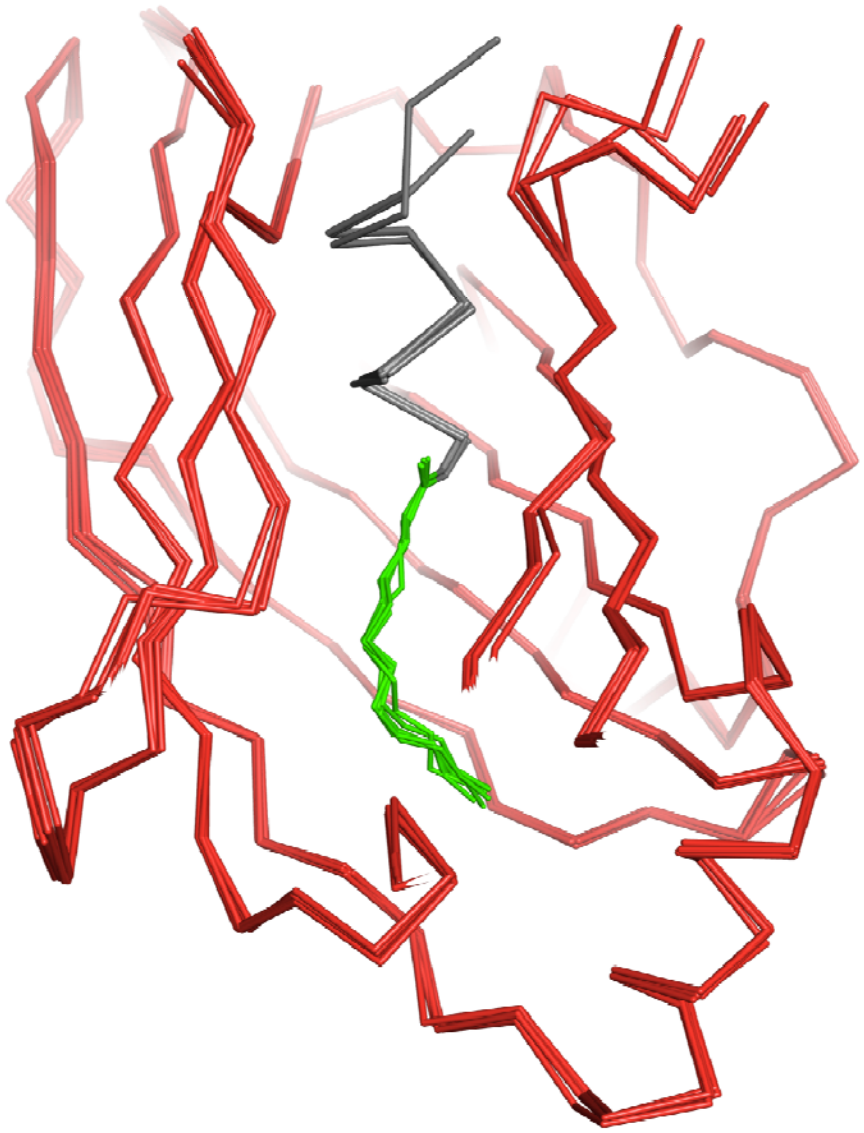

Figure S3 Overlap of the UNC119 carbon-α coordinates and associated ligands. The UNC119 carbon-α coordinates for each of the six molecules in the asymmetric unit were overlapped and are shown in red. In each of the molecules the lauroyl-GAGASAEEKH ligand is bound in very similar fashion. The acyl group of the ligand is shown in green and the ordered peptide residues of the ligand are colored gray. Figure created with PyMOL (www.pymol.org).

Nature Neuroscience: doi:10.1038/nn.2835

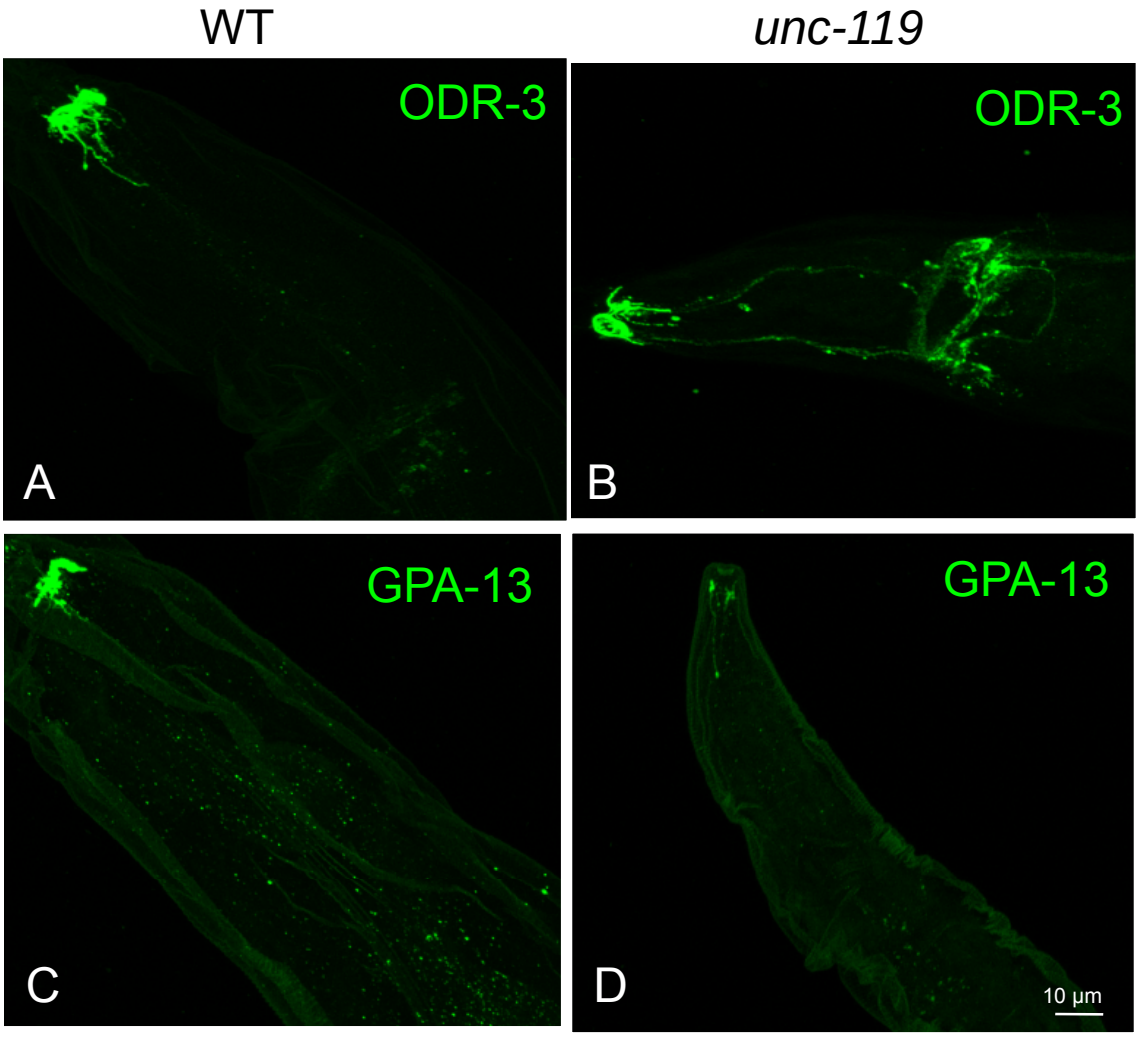

Figure S4 A–D ODR-3 and GPA-13 trafficking defects in mutant *C. elegans* olfactory neurons. (**A–D**), localization of ODR-3 (A, B) and GPA-13 (C,D) in wild-type (A,C) and *unc-119* mutant (B,D) *C. elegans* olfactory neurons. In wild-type neurons, ODR-3 and GPA-13 (green) traffic normally to the olfactory cilia. In mutant neurons, the G protein subunits are mislocalized (B, ODR-3) or exhibit decreased expression (D, GPA-13).

Nature Neuroscience: doi:10.1038/nn.2835

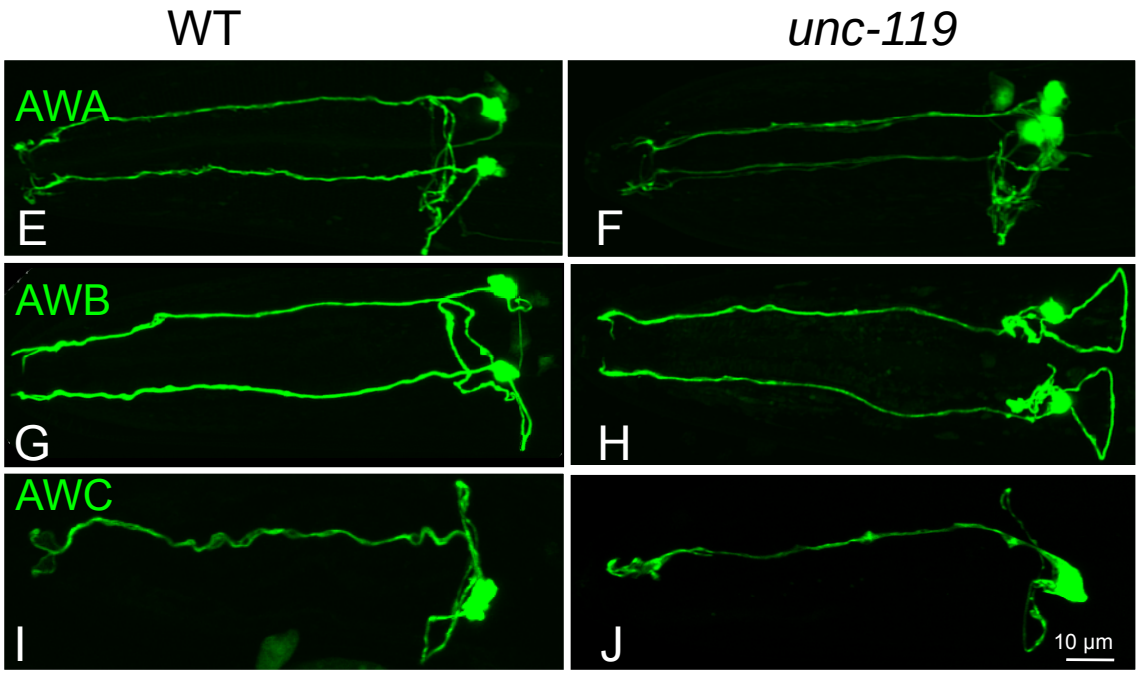

Figure S4 E–J ODR-3 and GPA-13 trafficking defects in mutant *C. elegans* olfactory neurons. **E–J**, structural Integrity of AWA, AWB and AWC Cilia in *unc-119 C. elegans* and restoration of ODR-3 and GPA-13 Localization. GFP was specifically expressed in AWA neurons (E,F), AWB neurons (G,H), and AWC neurons (I,J) of wild-type (left column) and *unc-119* mutant (right column) *C. elegans* worms. Reporter constructs were odr-10::gfp for AWA, str-1::GFP for AWB, and str-2::GFP for AWC. The structural integrity of these neurons is not compromised in the mutant (F,H,J) when compared to WT (E,G.I). Please note that transgene *kyIs140* in the *unc-119* mutant background only expressed GFP in one of the two AWC neurons (**Fig. S4I,J**), while some of the transgenic worms expressed GFP in both AWC neurons (unpublished data). Similar phenomena have been reported for other mutants (Troemel et al., *Cell* **99**, 387-398 (1999).

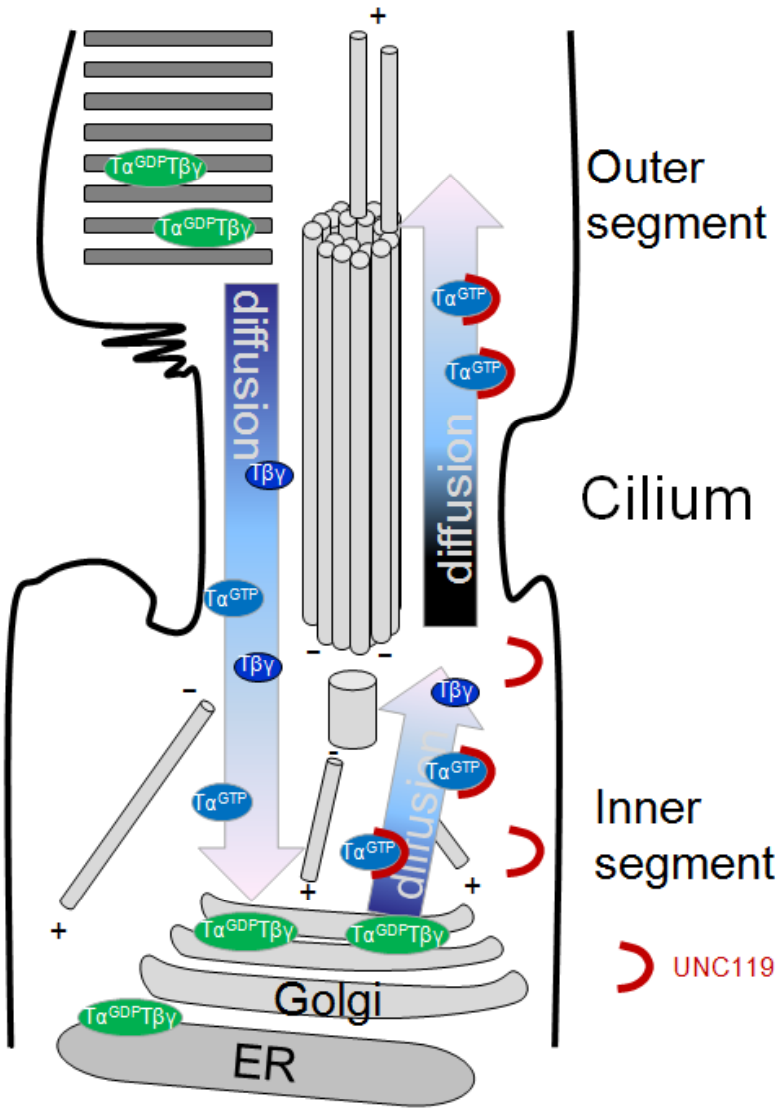

Fig. S5 Light-induced translocation of transducin and return to the outer segment. (**A**) Schematic depiction of transducin translocation. Under intense light, $T\alpha^{GTP}$ and Tβγ translocate separately to the inner segment and following GTP hydrolysis, associate with inner segment membranes as a heterotrimer $T\alpha^{GDP}\beta\gamma$. Following GDP/GTP exchange, which is very slow in the absence of rhodopsin, $T\alpha^{GTP}$ is eluted from the membrane by the acyl-binding protein UNC119. Tβγ elutes and associates with a prenyl binding protein, either PrBP/δ or phosducin[37]. Both Tα/UNC119 and Tβγ/PrBP diffuse freely and re-associate with a destination membrane after GTP hydrolysis. The destination membrane could be the cell membrane at the distal inner segment where IFT cargo is assembled or one of many outer segment disks.

Nature Neuroscience: doi:10.1038/nn.2835

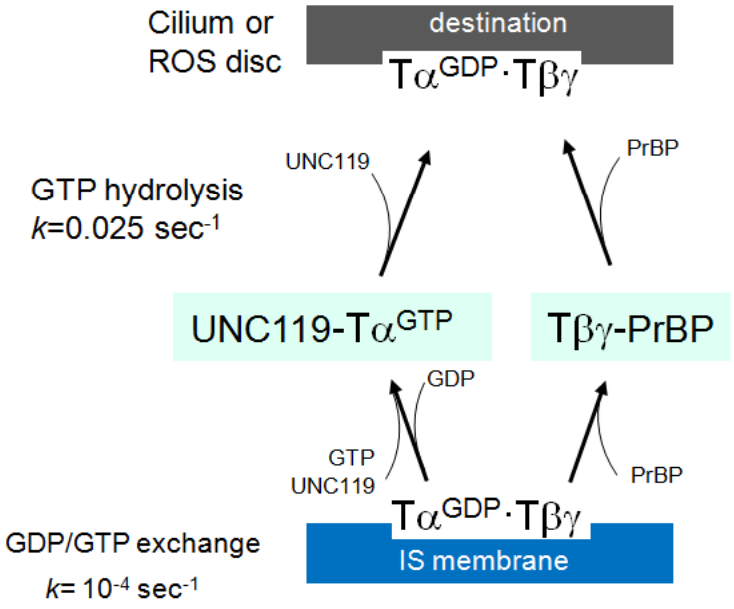

Fig. S5 Light-induced translocation of transducin and return to the outer segment. (**B**) Kinetic analysis of return to the OS. In the absence of a GEF (rhodopsin), solubilization of Tα governed by GDP/GTP exchange is slow (k= 10^{-4}/sec)[38], and is most likely the rate limiting step for the return of transducin. Likewise, the hydrolysis of $T\alpha^{GTP}$ is slow (k=0.025 sec^{-1}) in the absence of GAP, but not rate-limiting. GDP/GTP exchange maintains a rate constant of 0.0001/sec, resulting in only 0.01% of Tα solubilized per second [38], or one-third of Tα/hour, which explains the slow return to the outer segment.

Nature Neuroscience: doi:10.1038/nn.2835

Reference List

1. Hanzal-Bayer,M., Renault,L., Roversi,P., Wittinghofer,A., & Hillig,R.C. The complex of Arl2-GTP and PDE delta: from structure to function. *EMBO J.* **21**, 2095-2106 (2002).
2. Troemel,E.R., Sagasti,A., & Bargmann,C.I. Lateral signaling mediated by axon contact and calcium entry regulates asymmetric odorant receptor expression in C. elegans. *Cell* **99**, 387-398 (1999).